c-Myc and eIF4F Are Components of a Feedforward Loop that Links Transcription and Translation

Chen-Ju Lin,[1] Regina Cencic,[1] John R. Mills,[1] Francis Robert,[1] and Jerry Pelletier[1,2]

[1]Department of Biochemistry and [2]McGill Cancer Center, McGill University, Montreal, Quebec, Canada

Abstract

The Myc/Max/Mad family of transcription factors and the eukaryotic initiation factor 4F (eIF4F) complex play fundamental roles in regulating cell growth, proliferation, differentiation, and oncogenic transformation. eIF4F is involved in the recruitment of ribosomes to mRNAs and is thought to generally be the rate-limiting phase of translation. Here, we show that c-Myc directly activates transcription of the three subunits of eIF4F (eIF4E, eIF4AI, and eIF4GI). These transcriptional effects are mediated through canonical E-boxes (5′CACGTG3′) present in the promoters of these genes. In addition, the c-Myc antagonist Mad1 down-regulates the expression of eIF4F subunits. We also show that MycER activation stimulates protein synthesis at the level of translation initiation. Increased eIF4F levels result in stimulation of c-Myc mRNA translation specifically, as assessed by quantitative reverse transcription–PCR. We use a murine model of lymphomagenesis to show the expression of eIF4F subunits is also up-regulated by c-Myc *in vivo*. Our results suggest the presence of a feedforward loop involving c-Myc and eIF4F that serves to link transcription and translation and that could contribute to the effects of c-Myc on cell proliferation and neoplastic growth. [Cancer Res 2008;68(13):5326–34]

Introduction

The MAX network of transcription factors is composed of a group of basic helix-loop-helix and leucine-zipper (bHLH-Zip) proteins that form heterodimers with the bHLH-Zip protein MAX (1). These proteins include the Myc family of activators and the Mad family of repressors. Both Myc and Mad family members bind DNA to E-box sequence motifs (5′CACGTG3′ and related sequences), thereby modulating the transcriptional activity of genes that play critical roles in the regulation of cell growth, proliferation, differentiation, and apoptosis (1). c-Myc protein expression is rapidly induced upon mitogenic stimulation and down-regulated during cellular differentiation. Alterations of the c-Myc locus, caused by chromosomal translocation, amplification, or retroviral insertion, lead to deregulated c-Myc expression and contribute to tumorigenesis (1). In contrast to c-Myc, Mad protein members are expressed in differentiating and resting cells and are negative regulators of cell growth. Mad1 inhibits cell cycle progression, apoptosis, and transformation of tumor cells (2).

Drosophila and mammalian Myc have been implicated in promoting cell growth and protein synthesis (3, 4)—events also associated with increased translation factor production. For example, increases in eukaryotic initiation factor 4E (eIF4E) and eIF4A mRNA and protein levels occur after stimulation of resting lymphocytes to proliferate (5) and during liver regeneration (6). Consistent with these observations, recent identification of c-Myc target genes by chromatin immunoprecipitation (ChIP) and cDNA microarrays has revealed that expression of up to 15% of all genes may be affected by c-Myc, including many involved in ribosome biogenesis and protein synthesis (7, 8). Among translation initiation factors identified as c-Myc targets are eIF4E, eIF4AI, eIF4GI, and eIF4B (8–10). However, with the exception of eIF4E, none of these have been validated nor has the functional significance of this regulation been addressed. eIF4E is a well-characterized target of c-Myc, and transactivation is mediated by the presence of two E-box motifs in the eIF4E promoter (11). eIF4E and eIF2α expression increases after induction of growth in fibroblasts by c-Myc and suggests that c-Myc may regulate translation initiation (12).

The recruitment of ribosomes to the 5′ end of mRNAs during translation initiation in eukaryotic cells is generally thought to be the rate-limiting step of protein synthesis (13). Cap-dependent translation initiation is stimulated by eIF4F, a heterotrimeric complex that binds to the 5′ cap structure (m^7GpppX, where X is any nucleotide) of mRNAs. eIF4F is composed of three subunits: (*a*) eIF4E, which interacts directly with the mRNA cap structure in an ATP-dependent fashion; (*b*) eIF4A, an RNA helicase that prepares the mRNA template for ribosome binding; and (*c*) eIF4G, a molecular scaffold that mediates mRNA binding of the 43S preinitiation complex (40S ribosome and associated factors). eIF4B stimulates the helicase activity of eIF4A. eIF4F plays a key role in regulating cell growth, protein synthesis, and cell cycle progression (13).

Deregulated protein synthesis is emerging as a key event in human oncogenesis. Increased eIF4F activity (14) and ectopic expression of eIF4E, eIF4GI, and some eIF3 subunits can transform cells in culture (15–17). Overexpression of eIF4E cooperates with c-Myc *in vivo* (18) by antagonizing proapoptotic activities of c-Myc (19, 20), induces drug resistance, and is a genetic modifier of the rapamycin response (21). To gain insight into the potential regulation of translation initiation by c-Myc, we investigated whether eIF4AI and eIF4GI are c-Myc target genes. We show that the role of c-Myc during cell growth and proliferation is linked to an increase in eIF4F activity in a feedforward relationship, thus providing a possible molecular mechanism of cell transformation by c-Myc.

Materials and Methods

Retroviral infection, cell lines, and cell culture. The retroviral vectors, pBabePuro, pBabePuro-Mad1, and pBabePuro-MycER were transiently

Note: Supplementary data for this article are available at Cancer Research Online (http://cancerres.aacrjournals.org/).

Requests for reprints: Jerry Pelletier, McIntyre Medical Sciences Building, Room 810, 3655 Promenade Sir William Osler, McGill University, Montreal, Quebec, H3G 1Y6, Canada. Phone: 514-398-2323; Fax: 514-398-7384; E-mail: jerry.pelletier@mcgill.ca.

doi:10.1158/0008-5472.CAN-07-5876

transfected into the Phoenix-packaging cell line by using the calcium phosphate method. Recombinant retroviruses were harvested 48 to 60 h posttransfection and used to infect NIH3T3 cells in the presence of 8 μg/mL polybrene. Pools of resistant colonies were generated by selection in 2 μg/mL puromycin for 2 wk. For c-Myc induction, 80% confluent MycER cells were serum-starved for 24 h in DMEM supplemented with 0.5% fetal bovine serum (FBS), and 4-hydroxytamoxifen (4-OHT; Sigma) was added to a final concentration of 250 nmol/L for the indicated time periods. Where specified, cycloheximide (Sigma) was added at 10 μg/mL for 30 min before addition of 4-OHT.

Plasmid constructions. The source and construction of plasmids used in this study are described in the supplementary data.

Northern blot analysis. Total RNA was extracted from cells using TRIzol (Invitrogen). RNA was electrophoresed in a 1% formaldehyde-agarose gel and transferred to Hybond N+ membrane (GE Healthcare). Hybridizations were performed in ExpressHyb (Clontech) at 68°C with ^{32}P-labeled probes (1×10^6 cpm/mL) prepared with α-[^{32}P]dCTP using RTG DNA Beads (Amersham). Autoradiography of the membrane was performed at −80°C with film (Kodak X-Omat). Signal intensities were determined on a phosphorimager (Fuji-BAS 1000). Preparation of the probes is described in the supplementary data.

Nuclear run-on assays. Isolation of nuclei and nuclear run-on reactions were performed, as previously described (22), with slight modifications. The radiolabeled RNA was isolated using TRIzol reagent (Invitrogen). The final RNA pellet was dissolved in 50% formamide. Using a slot blot hybridization system with Hybond N+ nylon membranes, 2.5 μg of immobilized cDNA target were hybridized with equal numbers of counts ($1–2 \times 10^6$ cpm) of the labeled RNA. Prehybridization and hybridization of membranes was performed in ExpressHyb (Clontech) at 68°C. Autoradiography of the membrane was performed at −80°C with film (Kodak X-Omat). Signal intensities were quantitated with a phosphorimager (Fuji-BAS 2000).

Western blot analysis. Cells were harvested in radioimmunoprecipitation assay buffer [50 mmol/L Tris-HCl$_{7.5}$, 150 mmol/L NaCl, 1 mmol/L DTT, 0.1% SDS, 1% NP40, 0.5% sodium deoxycholate, 0.1 mmol/L phenylmethylsulfonyl fluoride (PMSF), 1 μg/mL each of leupeptin, pepstatin, and aprotinin]. Protein concentrations were quantified using a Bio-Rad protein assay and immunoblotting performed on 40 μg of total protein. After SDS-PAGE, proteins were transferred to polyvinylidene difluoride membranes (Millipore) and analyzed using the indicated antisera and enhanced chemiluminescence detection (Perkin-Elmer). The following antibodies were used: mouse anti-eIF4E (BD), anti-eIF4A (Santa Cruz), anti–α-tubulin (Sigma), rabbit anti-MAD1 (Santa Cruz), anti–c-MYC (Santa Cruz), and anti-eIF4GI (Bethyl).

7-Methyl-GTP-Sepharose pull-down. Cells were harvested in two volumes of hypotonic buffer A (25 mmol/L HEPES$_{7.5}$, 50 mmol/L KCl, 1.5 mmol/L MgCl$_2$, 1 mmol/L DTT, and 1 mmol/L PMSF), put on ice for

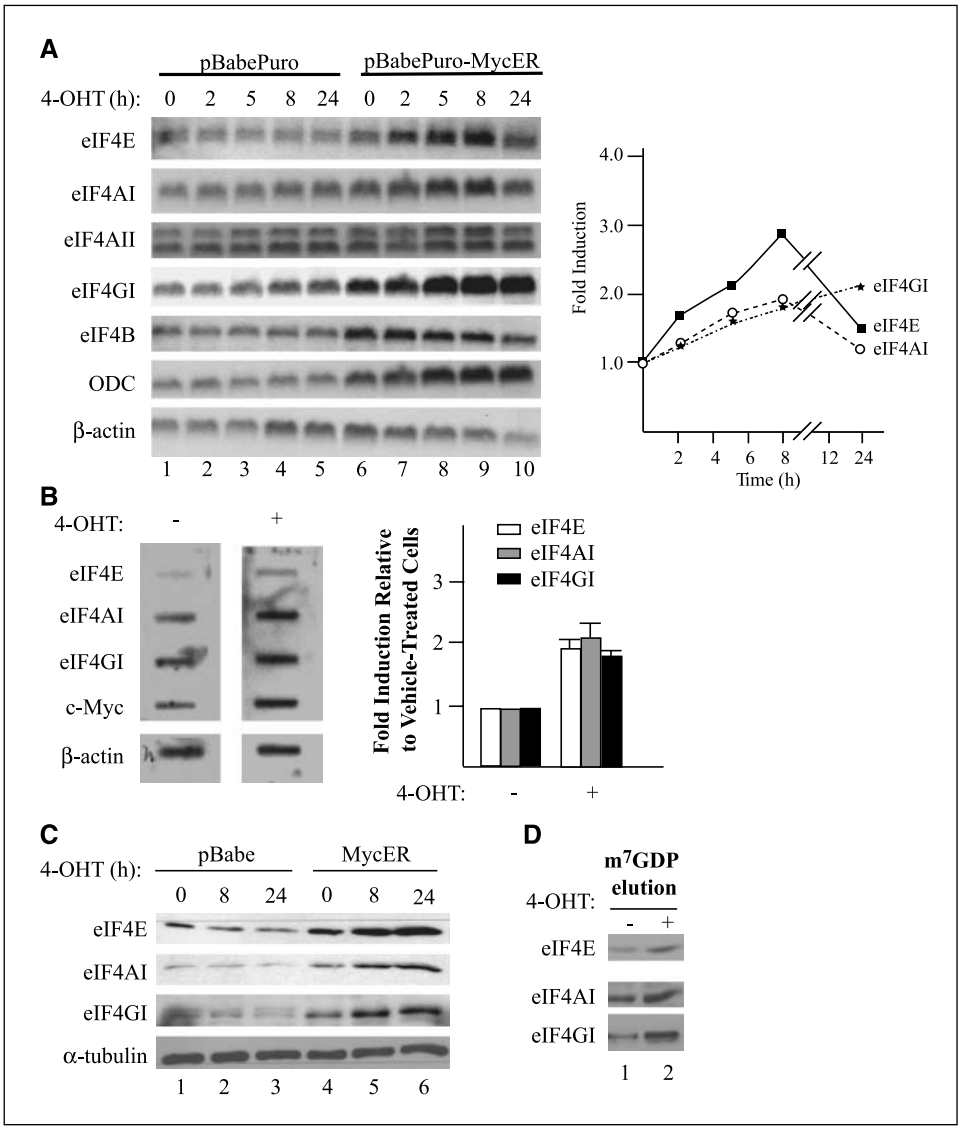

Figure 1. c-Myc up-regulates eIF4E, eIF4AI, and eIF4GI mRNA and protein levels. *A,* pBabePuro-infected and pBabePuro-MycER–infected NIH3T3 cells were incubated with 250 nmol/L 4-OHT for 2 to 24 h. Total RNA was analyzed by Northern blot (*left*) with indicated probes. The fold increase in eIF4E, eIF4AI, and eIF4GI mRNA levels, relative to *t* = 0 h (4-OHT; *lane 6*) and standardized to β-actin, is provided to the right and represents the average of four experiments. *B,* nuclear run-on analysis of eIF4E, eIF4AI, eIF4GI, and c-Myc gene transcription from pBabePuro-MycER cells treated with or without 250 nmol/L 4-OHT for 2 h. Note that the β-actin control hybridizations were performed in the same experiment as the others, but positioned more distal on the blot. Quantification (normalized to β-actin) is set relative to vehicle-treated cells and represents the average of three independent experiments with the error of the mean provided. *C,* pBabePuro and pBabePuro-MycER cells were treated with 250 nmol/L 4-OHT for 8 and 24 h. Extracts were analyzed by Western blotting with indicated antibodies. *D,* extracts prepared from pBabePuro-MycER cells treated with vehicle or 4-OHT were incubated with m^{7}GTP-coupled Sepharose resin, washed, and eIF4F-eluted with m^{7}GDP. Aliquots of the eluted fractions (25 μL) were analyzed by Western blotting with indicated antibodies.

20 min, then subjected to 20 strokes with a Dounce homogenizer. One milligram of cell extract was then incubated with 50 μL of 50% slurry of 7-methyl-GTP-Sepharose 4B (GE Healthcare) for 2 h at 4°C. The resin was washed thrice with 1 mL of buffer A containing 200 μmol/L GDP. Finally, proteins bound to the resin were eluted with 100 μL of m^7GDP (200 μmol/L) for 10 min on ice. Aliquots of the eluted fractions (25 μL) were resolved by SDS-PAGE (10% polyacrylamide) and analyzed by Western blotting.

Transfection and luciferase reporter assays. For transient transfection, 1.5×10^5 cells were seeded in 6-well plates at ~12 to 24 h before transfections. Transfections were performed with Lipofectamine and plus reagent (Invitrogen) with 0.2 μg of the firefly luciferase (FL) reporter plasmids, 1.2 μg of expression plasmids, and 20 ng of pcDNA3-*Renilla* luciferase (RL) as an internal control per well. Six hours posttransfection, cells were rinsed once with PBS and incubated with DMEM containing 10% FBS for an additional 40 h. MycER cells were treated with 4-OHT at 250 nmol/L for another 24 h. Cells were harvested, and luciferase activities were determined using the Promega dual luciferase assay kit.

ChIP. ChIP was performed as described in the supplementary data.

Polysome analysis and quantitative reverse transcription–PCR. Polysome analyses were performed on $\sim 2 \times 10^7$ MycER cells or 5×10^7 lymphomas for each gradient. Total RNA from the recovered fractions was isolated using TRIzol (Invitrogen). The amount of c-Myc mRNA was detected by quantitative reverse transcription–PCR (qRT-PCR) using the Roche Diagnostics LightCycler instrument and LightCycler RNA master SYBR green I kit according to the manufacturer's instruction. Known quantities of *in vitro* transcribed c-Myc template RNA served to generate a standard curve to determine the amount of RNA in each fraction. The primers used for qRT-PCR were 5′TGCGACTGACCCAACATCAG3′ and 5′CCTGTCCTGGCTCGCAGATT3′.

Isolation of B cells from mouse spleens is described in the supplementary data. The levels of c-Myc, eIF4E, eIF4AI, and eIF4GI mRNA from purified B cells isolated from Eμ-myc mice and normal littermates were measured by qRT-PCR. The primer sets are described in the supplementary data. All mRNA quantifications were normalized to β-actin.

Short hairpin RNA–mediated eIF4E knockdown. A template used to generate a short hairpin RNA (shRNA) construct against eIF4E was designed and described in the supplementary data.

Results

eIF4AI and eIF4GI are c-Myc responsive genes. The three subunits of eIF4F have been reported to be under regulation of c-Myc in previously reported microarray screens and ChIP (10, 23).[3] With the exception of eIF4E, the eIF4AI and eIF4GI genes have never been validated as c-Myc targets. Therefore, we used an inducible MycER system in NIH3T3 cells to systematically assess the expression kinetics of eIF4E, eIF4AI, and eIF4GI upon c-Myc activation (24). NIH3T3 cells were infected with pBabePuro or pBabePuro-MycER. The MycER fusion protein is an inducible system where c-Myc is fused to the hormone binding domain of the estrogen receptor. RNA extracted from serum-deprived cells at various time points after MycER activation was analyzed by Northern blotting. eIF4E, eIF4AI, and eIF4GI mRNA expression was induced upon MycER activation, but not eIF4AII or eIF4B (Fig. 1*A*). We note the presence of two eIF4AII isoforms, likely due to the use of alternative polyadenylation signals (25). Maximal induction of eIF4E, eIF4AI, and eIF4GI mRNAs was ~1.9-fold to 2.8-fold and observed 8 hours after 4-OHT addition (Fig. 1*A*, compare *lanes 6–10* with *lanes 1–5*). As a positive control, the known c-Myc target gene, ornithine decarboxylase mRNA, was also induced by MycER activation (Fig. 1*A*; ref. 26). Vehicle (ethanol) treatment of MycER cells did not induce eIF4E, eIF4AI, or eIF4GI mRNA levels (data not shown).

We also activated MycER with 4-OHT in the presence of cycloheximide. Cycloheximide alone increased the basal levels of eIF4E and eIF4AI mRNAs and decreased the levels of eIF4GI mRNA (Supplementary Fig. S1). However, addition of 4-OHT and CHX increased eIF4E, eIF4AI, and eIF4GI expression levels above those induced by cycloheximide alone (Supplementary Fig. S1). This suggests that c-Myc induction of eIF4E, eIF4AI, and eIF4GI is direct in that it does not require *de novo* protein synthesis.

To confirm that c-Myc was exerting its effect directly at the transcriptional level on the eIF4AI and eIF4GI promoter, we performed nuclear run-on analysis (Fig. 1*B*). After induction of MycER, nuclear run-on studies showed a reproducible 2-fold increase in eIF4AI and eIF4GI transcription rates compared with control cells (4-OHT; Fig. 1*B*). The eIF4E, eIF4AI, and eIF4GI protein levels were also up-regulated in response to MycER activation (Fig. 1*C*); however, 4-OHT treatment had no effect in pBabePuro-infected control cells (Fig. 1*C*, compare *lanes 4–6* with *lanes 1–3*). To address if increased production of eIF4F subunits resulted in elevated eIF4F complex formation, m^7GTP pull-down assays using MycER cells were performed. Analysis of the m^7GTP eluents revealed increased levels of the eIF4F complex in extracts prepared from 4-OHT–treated MycER NIH3T3 cells compared with vehicle-treated (Fig. 1*D*), indicating that c-Myc stimulates formation of the eIF4F complex.

We next examined a physiologic context in which c-Myc levels were altered to assess what response this would have on eIF4E, eIF4AI, and eIF4GI expression. To this end, we stimulated growth in fibroblasts with either serum or platelet-derived growth factor (Supplementary Fig. S2). We observed a rapid increase in c-Myc mRNA by 2 hours and also noted a parallel increase in eIF4E, eIF4AI, and eIF4GI mRNA expression. These results indicate that c-Myc and all eIF4F subunit expression are elevated after growth stimulation.

The eIF4F complex is down-regulated by Mad1. Myc:Max complexes activate transcription, whereas Mad:Max complexes bind the same canonical sites and typically repress transcription (1). We therefore manipulated Mad levels to reduce Myc:Max complexes (Fig. 2). Proliferating NIH3T3 cells were infected with pBabePuro or pBabePuro-Mad1 retroviruses, and the expression of Mad1 was confirmed by Western blot analysis (Fig. 2*A*). Compared with pBabe-infected cells, the levels of eIF4E, eIF4AI, and eIF4GI proteins decreased in NIH3T3 cells overexpressing Mad1 (Fig. 2*A*). In addition, cells expressing Mad1 displayed reduced transcription of eIF4E, eIF4AI, and eIF4GI compared with control cells, as determined by nuclear run-on assays (Fig. 2*B*). Moreover, enforced expression of Mad1 in proliferating NIH3T3 cells reduced levels of the eIF4F complex, as assessed by m^7GTP affinity pull-down experiments (Fig. 2*C*). Taken together, these findings indicate that expression of eIF4E, eIF4AI, and eIF4GI are transcriptionally regulated by Mad1.

Transcriptional regulation of the eIF4AI and eIF4GI promoters by c-Myc and Mad1 is E-box dependent. The mouse eIF4E gene contains two E-box sites (5′CACGTG3′) in its promoter at positions −80 and −244 (Fig. 3*A*; ref. 11). A canonical E-box was identified at position −297 upstream of the murine eIF4AI transcription start site (25). The murine eIF4GI gene contains two canonical E-boxes, which are located at positions −7 and −76, and a third one positioned +282 in the intronic region of the 5′

[3] www.myccancergene.org

untranslated region between exons 1 and 2 (Fig. 3*A*). These E-boxes are also conserved in the human promoters of eIF4AI and eIF4AGI (data not shown).

To determine whether these E-boxes could mediate transcriptional regulation by c-Myc and Mad1, a series of luciferase reporter constructs were generated (Fig. 3*A*). We fused a region extending 803 bp upstream of the eIF4AI transcription start site to the luciferase (Luc) coding region (Fig. 3*A*, eIF4AI^{wt}/Luc). When cotransfected with either pBabePuro (negative control), pBabePuro-Myc, or pBabePuro-Mad1 into NIH3T3 cells, we observed increased luciferase expression in response to c-Myc (~2.0-fold) and decreased luciferase activity in response to Mad1 (Fig. 3*B*). Although deletion of the E-box caused a slight decrease in the basal transcriptional activity of the eIF4AI promoter, relative to eIF4AI^{wt}/Luc, responsiveness to c-Myc and Mad1 was lost (Fig. 3*B*). Ectopic expression of c-Myc and Mad1 was confirmed by Western blotting of cell extracts (Fig. 3*B, right*). Moreover, overexpression of c-Myc or Mad1 caused an increase (~1.9-fold) or decrease (~35%) in luciferase activity, respectively, in transient cotransfection assays with eIF4GI^{wt}/Luc (Fig. 3*B*). To determine the relative contribution of the E-boxes to this effect, three mutants were generated (Fig. 3*A, right*). eIF4GI^{mut1}/Luc responded to c-Myc and Mad1 in a fashion similar to that observed for eIF4GI^{wt}/Luc. eIF4GI^{mut2}/Luc and eIF4GI^{mut12}/Luc no longer were responsive to c-Myc or Mad1 (Fig. 3*B*), indicating that E-box 2 within the eIF4GI promoter is responsible for mediating transactivation by c-Myc and Mad1. Transient transfection of MycER cells with the eIF4AI and eIF4GI reporter constructs further indicated that transcriptional regulation of the eIF4AI and eIF4GI promoters by c-Myc is E-box dependent (Fig. 3*C*). Consistent with these results, introduction of a dominant negative c-Myc mutant (Myc/Br) down-regulated eIF4AI and eIF4GI promoter activities in transient cotransfection assays (Supplementary Fig. S3).

To directly confirm that c-Myc was bound to the eIF4AI and eIF4GI promoters *in vivo*, a ChIP assay using MycER cells was performed. c-Myc bound to the eIF4E, eIF4AI, and eIF4GI E-box–containing promoters after the addition of 4-OHT (Fig. 3*D*). Binding was detected as early as 2 h, and longer incubations did not lead to increased binding. Background controls using antibodies directed against p27 revealed that the precipitation was specific (Fig. 3*D*). We were unable to detect binding of Myc to the downstream coding regions of eIF4AI and eIF4GI (data not shown) or to the β-actin gene promoter (Fig. 3*D*). We conclude that MycER proteins interact *in vivo* with the E-box of the eIF4AI and eIF4GI promoter in a hormone-regulated manner.

c-Myc stimulates protein synthesis by up-regulating eIF4F. Activation of c-Myc function correlates with an increase in protein synthesis (27). Our observation that c-Myc regulates levels of eIF4E, eIF4AI, and eIF4GI suggests that c-Myc promotes cell growth by regulating the ribosome recruitment phase of translation initiation, the rate-limiting step in protein synthesis. Polysome analysis of MycER cells exposed to 4-OHT (Fig. 4*A, middle*) revealed an increase in polysomes and a reduction of free ribosomes compared with vehicle-treated cells (Fig. 4*A, left*). Activation of MycER was associated with increased protein synthesis in 4-OHT–treated cells, as determined by [^{35}S]methionine incorporation into TCA-insoluble material (Supplementary Fig. S4).

Previous reports indicated that Chinese hamster ovary cells transformed by eIF4E display increased c-Myc protein expression (28). We therefore assessed the status of endogenous c-Myc protein levels in response to MycER activation and found it to be increased (Fig. 4*B*). We then monitored the distribution of endogenous c-Myc mRNA in polysomes from vehicle-treated and 4-OHT–treated MycER cells (Fig. 4*C*). The endogenous c-Myc mRNA was distinguishable from MycER mRNA, with primers targeting the 5′ untranslated region, because this region was not present in the MycER expression vector. qRT-PCR indicated that c-Myc mRNA was shifted into heavier polysome fractions in 4-OHT–treated MycER cells (Fig. 4*C*, compare *fractions 20–24*). The distribution of β-actin was similar among the polysomes (Fig. 4*D*).

To address whether translation of c-Myc is eIF4E responsive *in vivo*, we knocked down eIF4E using an shRNA-based approach.

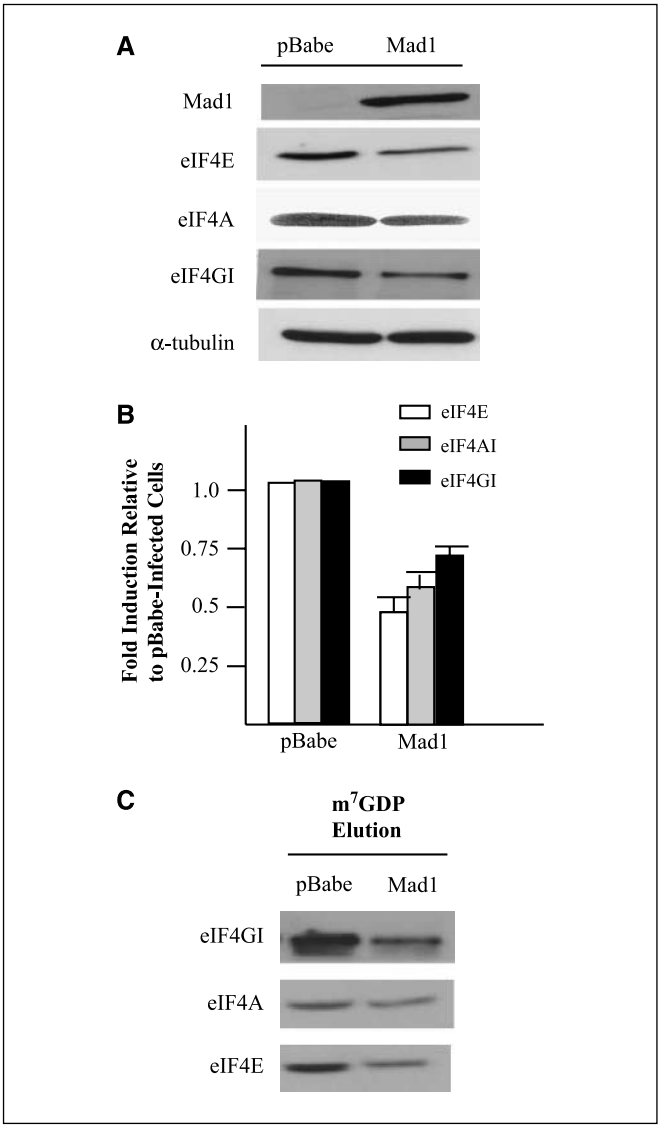

Figure 2. Expression of the eIF4F complex is down-regulated by Mad1. *A,* proliferating NIH3T3 cells were infected with pBabe or pBabe-Mad1 retrovirus, selected and analyzed by Western blot for expression of eIF4F subunits. *B,* the same cells, as in *A*, were analyzed for eIF4E, eIF4AI, and eIF4GI transcription by nuclear run-on assays. Quantification (normalized to β-actin) is set relative to pBabePuro-infected cells and represents the average of three independent experiments with the error of the mean provided. *C,* Western blot analysis of m^{7}GTP affinity pull-downs performed with cell extracts prepared from pBabePuro- or pBabePuro-Mad1–infected cells. Antibodies used were direct against the proteins (*left*).

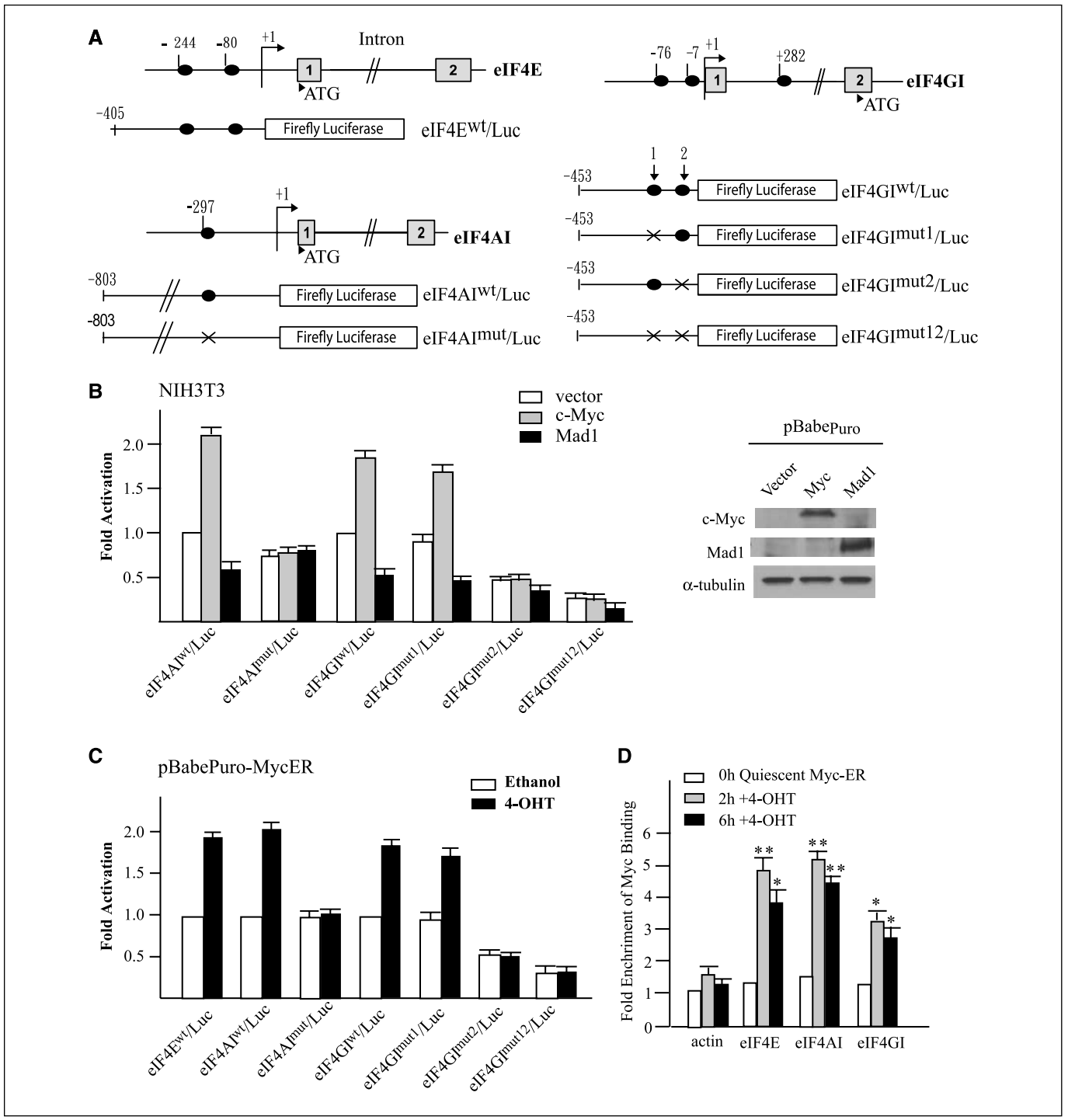

Figure 3. Activation of the eIF4AI and eIF4GI promoters by c-Myc is mediated by E-boxes. *A,* schematic diagram of the eIF4E, eIF4AI, and eIF4GI genomic regions. E-boxes are denoted by blackened ovals with the position relative to the transcription start site for each gene. For the murine eIF4GI mRNA, the denoted transcription start site corresponds to the human eIF4GI α promoter originating from exon 1 (Genbank NM_198241). *Gray squares,* exons; *arrowheads,* ATG codons. *B,* the indicated reporter constructs were transiently transfected into NIH3T3 cells with pcDNA3-RL, together with plasmids expressing c-Myc (*gray columns*) or Mad1 (*black columns*). Cells were harvested and assayed for firefly (FL) and *Renilla* (RL) activities. FL activities were expressed relative to wild-type reporter transfected with pBabePuro expression vector. *Columns,* average of FL/RL ratio of three independent experiments in duplicate; *bars,* SE. The blot to the right illustrates ectopic expression of c-Myc and Mad1, confirmed by Western blotting of cell extracts. *C,* MycER cells were transiently transfected with the indicated reporter plasmids and pcDNA3-RL. FL activities are expressed relative to wild-type reporter in the presence of vehicle. *Columns,* average of FL/RL ratio of three independent experiments performed in duplicate; *bars,* SE. *D,* quantitation of MycER binding to the eIF4E, eIF4AI, and eIF4GI promoters after addition of 4-OHT. Quiescent NIH3T3 cells expressing MycER were analyzed by ChIP before (*white columns*), 2 h (*gray columns*), and 6 h (*black columns*) after 4-OHT treatment. ChIP assays were performed using anti-Myc antibody or anti-p27 (as background control antibody) and the amount of immunoprecipitated DNA analyzed by quantitative real-time PCR. The graph shows fold enrichment over background signal (anti-p27 immunoprecipitation) as an average of duplicate PCRs from three independent experiments, with the error bars representing SE. The β-actin promoter does not contain E-boxes and served as a negative control. *, $P < 0.05$; **, $P < 0.01$ (calculated using Student's *t* test) compared with background signal obtained with anti-p27 immunoprecipitation.

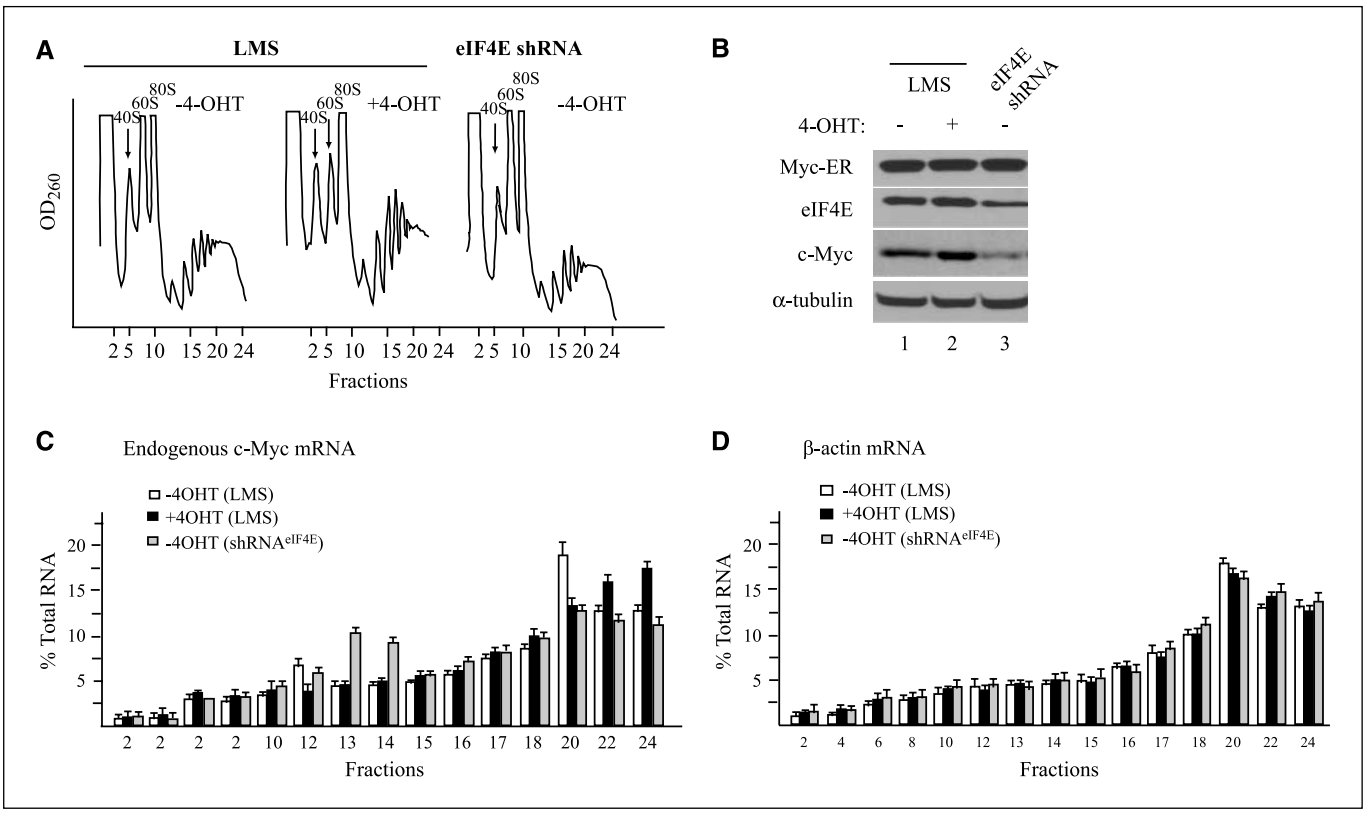

Figure 4. c-Myc expression stimulates endogenous c-Myc mRNA translation. *A,* polysome profiles obtained from LMS-infected MycER cells before (*left*) and after (*middle*) 4-OHT treatment or infected with a retrovirus carrying a shRNA to eIF4E (*right*). *B,* extracts prepared from MycER cells treated with vehicle (*lane 1*), 4-OHT (*lane 2*), or infected with a retrovirus carrying a shRNA to eIF4E (*lane 3*) were analyzed by Western blot with the indicated antibodies. *C* and *D,* RNA was purified from the indicated fractions in the polysome profile from *A* and quantified using qRT-PCR for c-Myc (*C*) and β-actin (*D*). The relative amount in each fraction is expressed as a percentage of its total in polysomes. The values are averaged from two independent experiments performed in duplicate and the error bars denote the error of mean ($n = 4$).

Knockdown of eIF4E did not affect global protein synthesis (Fig. 4*A, right* and Supplementary Fig. S4). This is consistent with the idea that modulating levels of eIF4E exerts gene-specific translational effects (29), and indeed eIF4E shRNA expressing cells displayed reduced c-Myc protein levels (Fig. 4*B*). A difference in the distribution of endogenous c-Myc mRNA was also evident in eIF4E knockdown cells, with the mRNA shifting its distribution into lighter fractions (Fig. 4*C, fractions 13 and 14*). These results indicate that endogenous c-Myc is under translational regulation when MycER expression is induced and that a proportion of c-Myc mRNA translation is eIF4E responsive.

Expression of eIF4F and c-Myc in a murine model of lymphomagenesis and HL-60 leukemia cells. Our results predict that in physiologic contexts where c-Myc levels are altered, we should observe changes in eIF4F subunit levels. We used an Eμ-myc transgenic model where c-Myc expression in pre-B cells is deregulated—leading to B-cell lymphoma development within 3 to 6 months after birth (30). RNA isolated from spleens of C57BL/6 and Eμ-Myc mice were analyzed by Northern blotting, which revealed increased levels of transcripts for all three eIF4F subunits (Fig. 5*A*). The increased mRNA levels were due to increased transcription rates, as determined by nuclear run-on assays (Fig. 5*B*). To address if this was an early event that occurred before oncogenic transformation and clonal selection, we isolated premalignant B cells from Eμ-Myc mice and used qRT-PCR to measure levels of eIF4E, eIF4AI, and eIF4GI mRNAs. We observed elevated eIF4E, eIF4AI, and eIF4GI mRNA levels in premalignant B cells of Eμ-Myc mice (Supplementary Fig. S5).

Eμ-myc mice carrying a lesion in the Tsc2 gene show accelerated lymphomagenesis compared with Eμ-myc mice.[4] Rapamycin treatment of *Tsc2*$^{-/-}$*Eμ-myc* lymphomas caused a reduction in translation initiation (Supplementary Fig. S6), which has been reported to be associated with a decrease in eIF4F activity.[4] qRT-PCR revealed that the distribution of c-Myc mRNA was shifted to lighter polysome fractions in rapamycin-treated *Tsc2*$^{-/-}$*Eμ-myc* lymphomas, whereas the distribution of β-actin mRNA remained unchanged (Fig. 5*C*). Rapamycin treatment caused a decrease in p-S6 levels indicative of mTORC1 inhibition, and we observed a corresponding reduction in c-Myc protein levels (Fig. 5*D*). We directly interfered with eIF4F activity with hippuristanol, a small molecule inhibitor of eIF4A (31), and found that c-Myc expression was also decreased in *Tsc2*$^{+/-}$*Eμ-myc* lymphomas (Supplementary Fig. S7). Taken together, these results suggest that the existence of a feedforward loop between c-Myc and eIF4F could contribute to lymphoma development.

Next, we evaluated HL-60 leukemia cell differentiation after exposure to 12-*O*-tetradecanoylphorbol-13-acetate, an event

[4] J. Mills, Y. Hippo, F, Robert, et al. mTORC1 is epistatic to Akt in the Eμ-MYC mouse model. PNAS. In press, 2008.

associated with decreased c-Myc and increased Mad1 levels (1). Northern blot analyses indicated that c-Myc mRNA was significantly reduced after 24 h and had completely disappeared by 48 h (Supplementary Fig. S8). Down-regulation of eIF4AI and eIF4GI mRNAs and proteins correlated with the decline in c-Myc mRNA (Supplementary Fig. S8*A* and *B*). These experiments are consistent with the eIF4F subunits being under regulation of members of the MAX network of transcription factors.

Discussion

Myc can regulate cell growth and protein synthesis (32). The absence of c-Myc in rat fibroblast cells markedly impairs protein synthesis (33), whereas up-regulation of c-Myc in a number of settings has striking effects on cell size and protein synthesis (3). For example, constitutive expression of a c-Myc transgene under control of the immunoglobulin heavy-chain enhancer increases the cell size of B lymphocytes at all stages of B-cell development, accompanied by an increase in protein synthesis (3). Consistent with these observations, many c-Myc target genes identified from global screening approaches are involved in protein synthesis and ribosome biogenesis (10). We show that, in addition to eIF4E (12), eIF4AI and eIF4GI are *bona fide* c-Myc targets. eIF4F levels are increased upon c-Myc activation (Fig. 1), which in turn positively regulates translation of c-Myc mRNA (Fig. 4). This suggests the presence of a feedforward loop involving c-Myc and eIF4F that links the processes of transcription and translation (Fig. 6).

ChIP analyses indicate that c-Myc transactivates eIF4AI by directly binding to the canonical E-box in the promoter regions (Fig. 3*D*). There are two functional eIF4A genes, eIF4AI and eIF4AII, which encode proteins with amino acid sequences that are 91% identical and functionally interchangeable *in vitro* (34). However, we did not find any E-boxes located within 2 kb on either side of transcription start sites of eIF4AII and eIF4AII mRNA levels remained unchanged upon MycER activation (Fig. 1*A*). These results are consistent with the fact that eIF4AI is 10 times more abundant than eIF4AII in growing cells, suggesting that c-Myc may be responsible for this differential regulation (35). Rosenwald and colleagues have reported unchanged eIF4A mRNA levels after MycER activation, but their failure to distinguish between the two

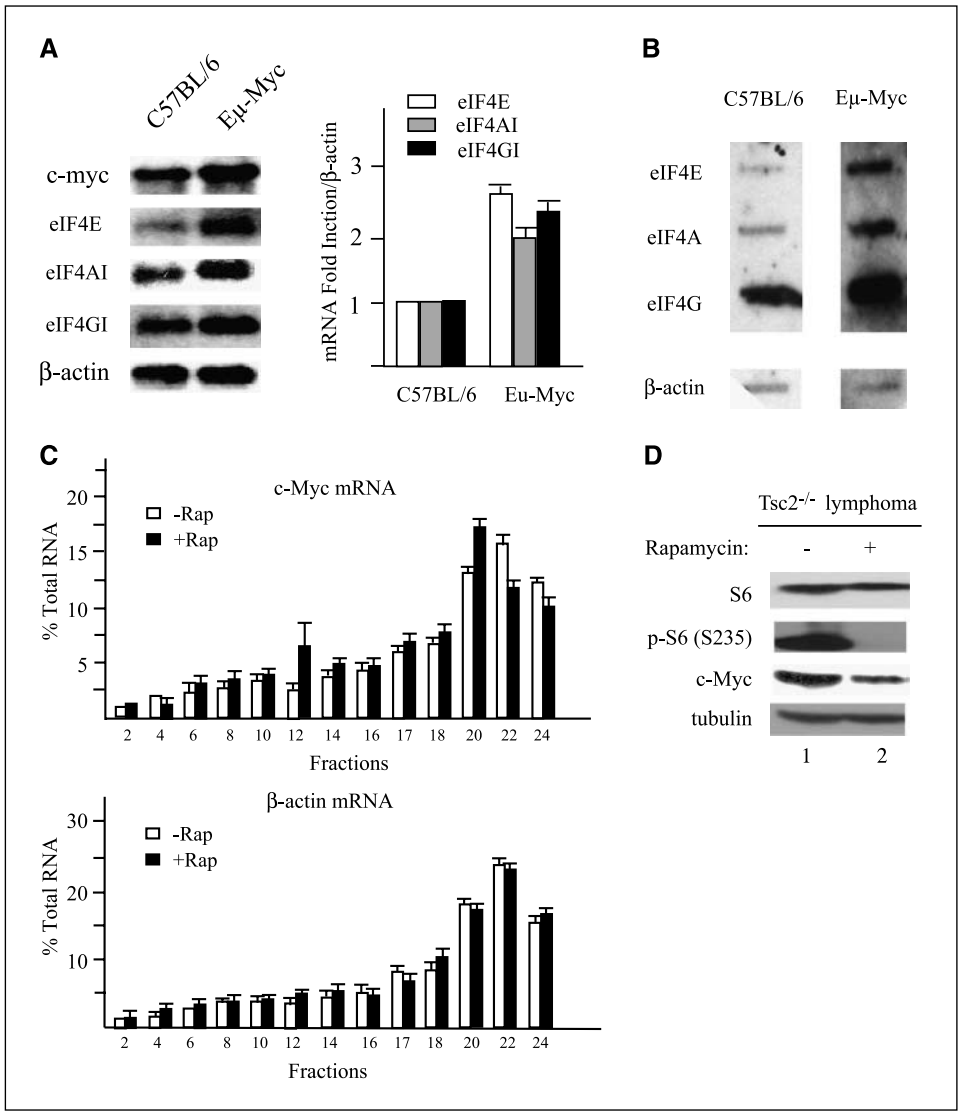

Figure 5. Expression of eIF4F and c-Myc in a murine model of lymphomagenesis. *A,* RNA was isolated from normal spleens and from Eμ-Myc spleen harboring lymphomas and was analyzed by Northern blot (β-actin control) with quantification expressed as a bar graph (*right*). *B,* nuclear run-on analysis of the eIF4E, eIF4AI, and eIF4GI genes in spleen of Eμ-Myc mice relative to C57BL/6 (note that in this experiment, the β-actin control is from the same membrane as the other probes, but was positioned more distal on the membrane). *C,* analysis of c-Myc and β-actin mRNA distribution across polysomes from vehicle-treated or rapamycin-treated (20 nmol/L) *Tsc2*$^{-/+}$*Eμ-myc* lymphomas. The relative amount of mRNA in each fraction is expressed as a percentage of the total in the polysome gradient. The values are averaged from two independent experiments performed in duplicate and the error bars denote the error of mean (n = 4). *D,* expression of c-Myc is reduced in *Tsc2*$^{-/+}$*Eμ-myc* lymphomas treated with rapamycin. Extracts prepared from *Tsc2*$^{-/+}$*Eμ-myc* lymphomas were analyzed by Western blot with indicated antibodies.

eIF4A isoforms may have masked selective changes in eIF4AI mRNA levels (12). eIF4B has also been identified as a potential c-Myc target gene by ChIP assays (9), but in our hands its expression did not change in response to MycER induction (Fig. 1*A*). These results highlight the importance of validating ChIP results and may suggest response differences to c-Myc among different cell lines or the presence of a second gene in the vicinity of the eIF4B locus that is regulated by c-Myc.

Alterations in the levels of the eIF4F subunits are associated with oncogenesis. eIF4E is a well-characterized transcriptional target of c-Myc (11), and elevated levels of eIF4E are transforming *in vitro* and *in vivo* (16, 18). Overexpression of eIF4GI in NIH3T3 fibroblasts produces cells that display anchorage-independent growth *in vitro* and form tumors *in vivo* (15). eIF4AI is overexpressed in melanoma (36) and hepatocellular carcinoma (37). One mechanism to explain the transforming potential of eIF4F has been attributed to translational remodeling of the oncoproteome resulting in a subsequent blockade of proapoptotic stimuli (19, 20).

eIF4F has been proposed to be rate-limiting for translation initiation *in vivo* and is a checkpoint for mTOR regulation (38). eIF4E is thought to be the least abundant subunit of the eIF4F complex (present at 0.3 molecules per ribosome), with eIF4G being present in approximately twice as many copies (0.5 copies per ribosome). eIF4A is the most abundant translation factor, being present at three copies per ribosome in exponentially growing cells (39). Why c-Myc should regulate the production of all three of these subunits is thus not apparent because increased production of eIF4E would conceptually be sufficient to increase eIF4F complex levels. Coordinated increases in the levels of all three subunits may be required for increased eIF4F complex formation if assembly of the complex is regulated. Formation of eIF4F is under mTOR regulation, with binding of eIF4E and eIF4A to repressor proteins regulated by phosphorylation events under mTOR regulation (40, 41). It remains to be established which activity or eIF4F subunit is (are) rate-limiting *in vivo*. It may be that all three factors are available at similar stoichiometric concentrations for translation initiation *in vivo*. Clearly, a decrease in eIF4E levels does not have a dramatic effect on global protein synthesis *in vivo* (Fig. 4*A* and Supplementary Fig. S4).

We observed that protein synthesis rates in MycER activated cells were ~2.2× higher than that of vehicle treated cells by [^{35}S]methionine pulse-labeling (Supplementary Fig. S4). To determine if the effect was at the level of translation initiation, polysome profiles were obtained from MycER cells treated with vehicle or 4-OHT. A shift toward heavier polysomes and a reduction in free ribosomes, relative to vehicle-treated cells, was observed upon MycER activation (Fig. 4*A*). This modest effect on translation can be accompanied by more pronounced consequences on the translation of a subset of mRNAs, as we show for c-Myc (Fig. 4*B* and *C*). Overexpression of eIF4E can preferentially stimulate translation of mRNAs containing secondary structure in their 5′ noncoding regions (42, 43).

c-Myc translation has been proposed to occur through cap-dependent and IRES-mediated translation, with the latter occurring during pathophysiologic cell stress (44). Our present data show that a proportion of c-Myc translation is also eIF4F-responsive (Fig. 4*C*), but this does not seem to be as severe as the observed reduction in c-MYC protein levels (Fig. 4*B*). We do not understand this, but cannot exclude that expression of a proportion of c-Myc mRNA that is still polysome-associated is repressed (e.g. by microRNA).

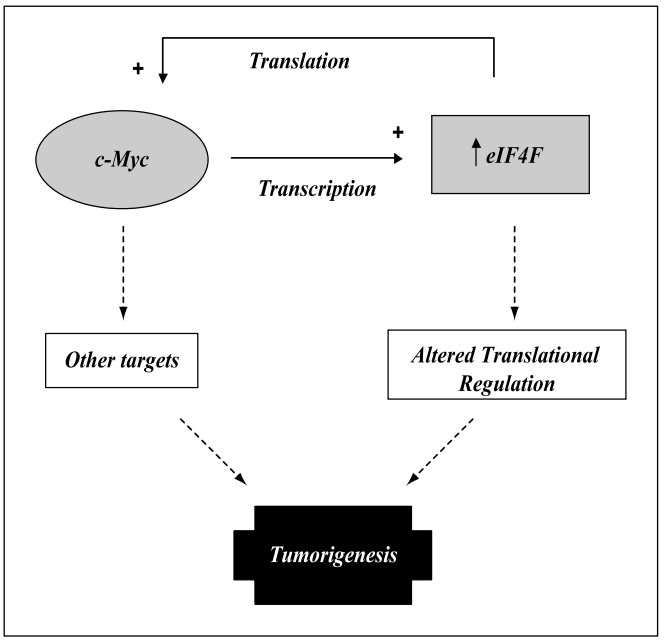

Figure 6. Model outlining a feedforward loop between c-Myc and eIF4F linking transcription and translation.

Our results indicate that the role of c-Myc during cell growth and proliferation is linked to an increase in eIF4F activity and suggests a mechanism whereby c-Myc stimulates protein synthesis by regulating the rate-limiting step of translation initiation. Increased eIF4F activity or levels contribute to aberrant cellular growth (14), implicating a role in the molecular mechanism of cell transformation by c-Myc. Regulators of transcription and translation that affect c-Myc function (e.g., Mad1) or eIF4F activity (e.g., mTOR) are expected to act as rheostats that fine tune the outcomes of the c-Myc/eIF4F feedforward loop. We find that eIF4F subunits are elevated in the Eμ-myc mouse model and rapamycin or hippuristanol treatment of *Tsc2*$^{-/+}$*Eμ-myc* lymphomas leads to a reduction in eIF4F activity, which in turn is associated with a decrease in c-Myc protein levels (Fig. 5 and Supplementary Fig. S7). A previous report also showed decreased c-Myc expression after exposure of EBV immortalized B cells to rapamycin (45). Uncoupling of the feedforward loop by mutational analysis or perturbations due to ectopic expression of factors would circumvent these checkpoints and could represent mechanisms that fuel neoplastic growth.

Disclosure of Potential Conflicts of Interest

No potential conflicts of interest were disclosed.

Acknowledgments

Received 10/14/2007; revised 4/22/2008; accepted 4/23/2008.

Grant support: Canadian Institutes of Health Research operating grant MOP-11354 (J. Pelletier).

The costs of publication of this article were defrayed in part by the payment of page charges. This article must therefore be hereby marked *advertisement* in accordance with 18 U.S.C. Section 1734 solely to indicate this fact.

We thank Drs. R.D. Hannan (Peter MacCallum Cancer Center), R.N. Eisenman (Fred Hutchinson Cancer Research Center), and P. Farnham (University of California) for their kind gift of pBabePuro-MycER, pVZ1mad plasmid, and long terminal repeat Myc/BR, respectively, and A. Malina for the design of the mouse β-actin primers used for qRT-PCR in this study.

References

1. Grandori C, Cowley SM, James LP, Eisenman RN. The Myc/Max/Mad network and the transcriptional control of cell behavior. Annu Rev Cell Dev Biol 2000; 16:653–99.
2. Bejarano MT, Albihn A, Cornvik T, et al. Inhibition of cell growth and apoptosis by inducible expression of the transcriptional repressor Mad1. Exp Cell Res 2000;260: 61–72.
3. Iritani BM, Eisenman RN. c-Myc enhances protein synthesis and cell size during B lymphocyte development. Proc Natl Acad Sci U S A 1999;96:13180–5.
4. Johnston LA, Prober DA, Edgar BA, et al. *Drosophila* myc regulates cellular growth during development. Cell 1999;98:779–90.
5. Mao X, Green JM, Safer B, et al. Regulation of translation initiation factor gene expression during human T cell activation. J Biol Chem 1992;267: 20444–50.
6. Aloni R, Peleg D, Meyuhas O. Selective translational control and nonspecific posttranscriptional regulation of ribosomal protein gene expression during development and regeneration of rat liver. Mol Cell Biol 1992;12: 2203–12.
7. Orian A, van Steensel B, Delrow J, et al. Genomic binding by the *Drosophila* Myc, Max, Mad/Mnt transcription factor network. Genes Dev 2003;17:1101–14.
8. Fernandez PC, Frank SR, Wang L, et al. Genomic targets of the human c-Myc protein. Genes Dev 2003;17: 1115–29.
9. Mao DY, Watson JD, Yan PS, et al. Analysis of Myc bound loci identified by CpG island arrays shows that Max is essential for Myc-dependent repression. Curr Biol 2003;13:882–6.
10. Coller HA, Grandori C, Tamayo P, et al. Expression analysis with oligonucleotide microarrays reveals that MYC regulates genes involved in growth, cell cycle, signaling, and adhesion. Proc Natl Acad Sci U S A 2000; 97:3260–5.
11. Jones RM, Branda J, Johnston KA, et al. An essential E box in the promoter of the gene encoding the mRNA cap-binding protein (eukaryotic initiation factor 4E) is a target for activation by c-myc. Mol Cell Biol 1996;16: 4754–64.
12. Rosenwald IB, Rhoads DB, Callanan LD, et al. Increased expression of eukaryotic translation initiation factors eIF-4E and eIF-2 α in response to growth induction by c-myc. Proc Natl Acad Sci U S A 1993;90: 6175–8.
13. Hershey JW, BaM WC. Initiation of Protein Synthesis. Plainview (NY): Cold Spring Harbor Lab. Press; 2000.
14. Avdulov S, Li S, Michalek V, et al. Activation of translation complex eIF4F is essential for the genesis and maintenance of the malignant phenotype in human mammary epithelial cells. Cancer Cell 2004;5: 553–63.
15. Fukuchi-Shimogori T, Ishii I, Kashiwagi K, et al. Malignant transformation by overproduction of translation initiation factor eIF4G. Cancer Res 1997;57: 5041–4.
16. Lazaris-Karatzas A, Montine KS, Sonenberg N. Malignant transformation by a eukaryotic initiation factor subunit that binds to mRNA 5′ cap. Nature 1990; 345:544–7.
17. Zhang L, Pan X, Hershey JW. Individual overexpression of five subunits of human translation initiation factor eIF3 promotes malignant transformation of immortal fibroblast cells. J Biol Chem 2007;282: 5790–800.
18. Wendel H-G, de Stanchina E, Fridman JS, et al. Survival signalling by Akt and eIF4E in oncogenesis and cancer therapy. Nature 2004;428:332–7.
19. Li S, Takasu T, Perlman DM, et al. Translation factor eIF4E rescues cells from Myc-dependent apoptosis by inhibiting cytochrome *c* release. J Biol Chem 2003;278: 3015–22.
20. Polunovsky VA, Rosenwald IB, Tan AT, et al. Translational control of programmed cell death: eukaryotic translation initiation factor 4E blocks apoptosis in growth-factor-restricted fibroblasts with physiologically expressed or deregulated Myc. Mol Cell Biol 1996; 16:6573–81.
21. Wendel HG, Malina A, Zhao Z, et al. Determinants of sensitivity and resistance to rapamycin-chemotherapy drug combinations *in vivo*. Cancer Res 2006;66: 7639–46.
22. Greenberg ME, Ziff EB. Stimulation of 3T3 cells induces transcription of the c-fos proto-oncogene. Nature 1984;311:433–8.
23. Schlosser I, Holzel M, Murnseer M, et al. A role for c-Myc in the regulation of ribosomal RNA processing. Nucleic Acids Res 2003;31:6148–56.
24. Littlewood TD, Hancock DC, Danielian PS, et al. A modified oestrogen receptor ligand-binding domain as an improved switch for the regulation of heterologous proteins. Nucleic Acids Res 1995;23:1686–90.
25. Nielsen PJ, Trachsel H. The mouse protein synthesis initiation factor 4A gene family includes two related functional genes which are differentially expressed. EMBO J 1988;7:2097–105.
26. Bello-Fernandez C, Packham G, Cleveland JL. The ornithine decarboxylase gene is a transcriptional target of c-Myc. Proc Natl Acad Sci U S A 1993;90: 7804–8.
27. Rosenwald IB. Upregulated expression of the genes encoding translation initiation factors eIF-4E and eIF-2α in transformed cells. Cancer Lett 1996; 102:113–23.
28. De Benedetti A, Joshi B, Graff J, Zimmer SG. CHO cells transformed by the translation factor eIF4E display increased c-myc expression, but required overexpression of Max for tumorigenicity. Mol Cell Differ 1994;2:347–71.
29. Dever TE. Gene-specific regulation by general translation factors. Cell 2002;108:545–56.
30. Langdon WY, Harris AW, Cory S, Adams JM. The c-myc oncogene perturbs B lymphocyte development in E-mu-myc transgenic mice. Cell 1986;47:11–8.
31. Bordeleau M-E, Mori A, Oberer M, et al. Functional characterization of IRESes by an inhibitor of the RNA helicase eIF4A. Nat Chem Biol 2006;2:213–20.
32. Schmidt EV. The role of c-myc in cellular growth control. Oncogene 1999;18:2988–96.
33. Mateyak MK, Obaya AJ, Adachi S, Sedivy JM. Phenotypes of c-Myc-deficient rat fibroblasts isolated by targeted homologous recombination. Cell Growth Differ 1997;8:1039–48.
34. Yoder-Hill J, Pause A, Sonenberg N, Merrick WC. The p46 subunit of eukaryotic initiation factor (eIF)-4F exchanges with eIF-4A. J Biol Chem 1993;268: 5566–73.
35. Williams-Hill DM, Duncan RF, Nielsen PJ, Tahara SM. Differential expression of the murine eukaryotic translation initiation factor isogenes eIF4A(I) and eIF4A(II) is dependent upon cellular growth status. Arch Biochem Biophys 1997;338:111–20.
36. Eberle J, Krasagakis K, Orfanos CE. Translation initiation factor eIF-4A1 mRNA is consistently overexpressed in human melanoma cells *in vitro*. Int J Cancer 1997;71:396–401.
37. Shuda M, Kondoh N, Tanaka K, et al. Enhanced expression of translation factor mRNAs in hepatocellular carcinoma. Anticancer Res 2000;20:2489–94.
38. Cormier P, Pyronnet S, Salaun P, et al. Cap-dependent translation and control of the cell cycle. Prog Cell Cycle Res 2003;5:469–75.
39. Duncan R, Milburn SC, Hershey JW. Regulated phosphorylation and low abundance of HeLa cell initiation factor eIF-4F suggest a role in translational control. Heat shock effects on eIF-4F. J Biol Chem 1987;262:380–8.
40. Dorrello NV, Peschiaroli A, Guardavaccaro D, et al. S6K1- and βTRCP-mediated degradation of PDCD4 promotes protein translation and cell growth. Science 2006;314:467–71.
41. Hay N, Sonenberg N. Upstream and downstream of mTOR. Genes Dev 2004;18:1926–45.
42. Koromilas AE, Lazaris-Karatzas A, Sonenberg N. mRNAs containing extensive secondary structure in their 5′ non-coding region translate efficiently in cells overexpressing initiation factor eIF-4E. EMBO J 1992;11: 4153–8.
43. Graff JR, Zimmer SG. Translational control and metastatic progression: enhanced activity of the mRNA cap-binding protein eIF-4E selectively enhances translation of metastasis-related mRNAs. Clin Exp Metastasis 2003;20:265–73.
44. Stoneley M, Subkhankulova T, Le Quesne JP, et al. Analysis of the c-myc IRES; a potential role for cell-type specific trans-acting factors and the nuclear compartment. Nucleic Acids Res 2000;28:687–94.
45. West MJ, Stoneley M, Willis AE. Translational induction of the c-myc oncogene via activation of the FRAP/TOR signalling pathway. Oncogene 1998;17:769–80.

Correction: c-Myc and eIF4F Link Translation and Transcription

In the article on how c-Myc and eIF4F link translation and transcription in the July 1, 2008 issue of *Cancer Research* (1), there is an error in Fig. 4*C*. The corrected figure appears below.

1. Lin C-J, Cencic R, Mills JR, Robert F, Pelletier J. c-Myc and eIF4F are components of a feedforward loop that links transcription and translation. Cancer Res 2008;68: 5326–34.

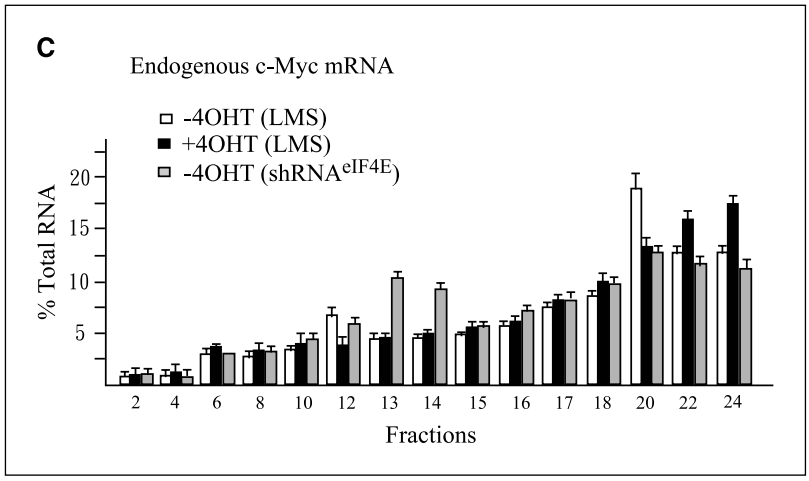

doi:10.1158/0008-5472.CAN-68-17-COR2

c-Myc and eIF4F Are Components of a Feedforward Loop that Links Transcription and Translation

Chen-Ju Lin, Regina Cencic, John R. Mills, et al.

Cancer Res 2008;68:5326-5334.